PALEOMAGNETIC POLES

The basic procedure for calculating a magnetic pole position is introduced here. Definitions of types of magnetic poles are then presented, leading to a discussion of paleomagnetic sampling of geomagnetic secular variation. Here you acquire methods for judging the next level of paleomagnetic analysis: the data set of site-mean directions and the paleomagnetic pole determined from those directions. Examples of paleomagnetic poles and some common-sense criteria for judging reliability of paleomagnetic poles are offered.

PROCEDURE FOR POLE DETERMINATION

The inclination and declination of a dipolar magnetic field change with position on the globe. But the position of the *magnetic pole* of a geocentric dipole is independent of observing locality. For many purposes, comparison of results between various observing localities is facilitated by determining a *pole position*. This pole position is simply the geographic location of the projection of the negative end of the dipole onto the Earth's surface, as shown in Figure 7.1.

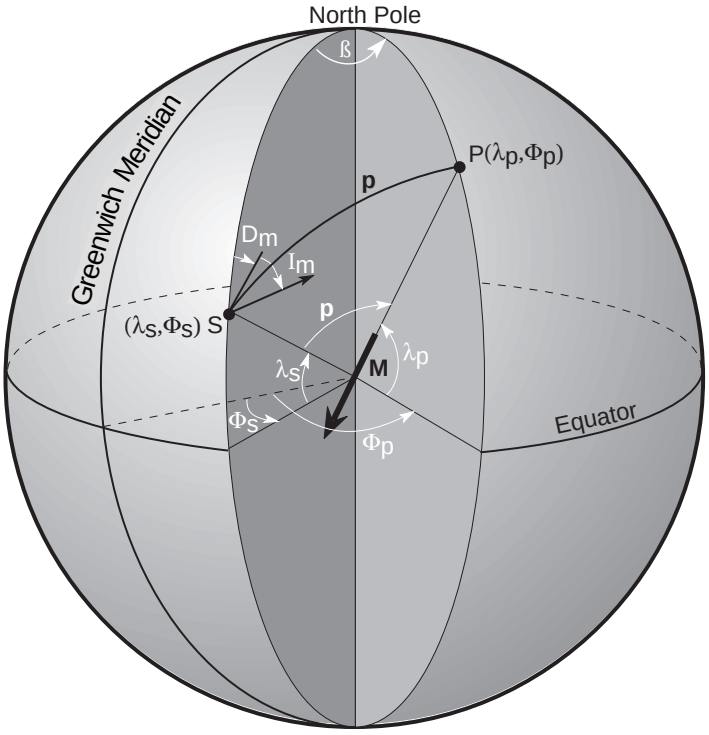

Figure 7.1 Determination of magnetic pole position from a magnetic field direction. Site location is at *S* (λ_s, ϕ_s); site-mean magnetic field direction is I_m, D_m; ***M*** is the geocentric dipole that can account for the observed magnetic field direction; *P* is the magnetic pole at (λ_p, ϕ_p); *p* is the magnetic colatitude (angular distance from *S* to *P*); North Pole is the north geographic pole; β is the difference in longitude between the magnetic pole and the site.

Calculation of a pole position is a navigational problem in spherical trigonometry that uses the dipole formula (Equation (1.15)) to determine the distance traveled from observing locality to pole position. Details of the derivation of a magnetic pole position from a magnetic field direction are given in the Appendix. Sign conventions for geographic locations are as follows:

1. Latitudes increase from –90° at south geographic pole to 0° at equator and to +90° at the north geographic pole.
2. Longitudes east of the Greenwich meridian are positive, while westerly longitudes are negative.

Figure 7.1 illustrates how a pole position (λ_p, ϕ_p) is calculated from a site-mean direction (I_m, D_m) measured at a particular site (λ_s, ϕ_s). The first step is to determine the magnetic *colatitude*, *p*, which is the great-circle distance from site to pole. From the dipole formula (Equation (1.15)),

$$p = \cot^{-1}\left(\frac{\tan I_m}{2}\right) = \tan^{-1}\left(\frac{2}{\tan I_m}\right) \tag{7.1}$$

Pole latitude is given by

$$\lambda_p = \sin^{-1}\left(\sin\lambda_s \cos p + \cos\lambda_s \sin p \cos D_m\right) \tag{7.2}$$

The longitudinal difference between pole and site is denoted by β, is positive toward the east, and is given by

$$\beta = \sin^{-1}\left(\frac{\sin p \sin D_m}{\cos\lambda_p}\right) \tag{7.3}$$

At this point in the calculation, there are two possibilities for pole longitude. If

$$\cos p \geq \sin\lambda_s \sin\lambda_p \tag{7.4}$$

then

$$\phi_p = \phi_s + \beta \tag{7.5}$$

But if

$$\cos p < \sin\lambda_s \sin\lambda_p \tag{7.6}$$

then

$$\phi_p = \phi_s + 180^{\circ} - \beta \tag{7.7}$$

Any site-mean direction I_m, D_m has an associated confidence limit α_{95}. This circular confidence limit about the site-mean direction is transformed (mapped by the dipole formula) into an ellipse of confidence about the calculated pole position (see Figure 7.2). The semi-axis of the ellipse of confidence has an angular length along the site-to-pole great circle given by

$$dp = \alpha_{95}\left(\frac{1+3\cos^2 p}{2}\right) \tag{7.8}$$

The semi-axis perpendicular to the great circle is given by

$$dm = \alpha_{95}\left(\frac{\sin p}{\cos I_m}\right) \tag{7.9}$$

As an example calculation, consider a site-mean direction I_m = 45°, D_m = 25° with α_{95} = 5.0° observed at location λ_s = 30°N, ϕ_s = 250°E (= 110°W). The colatitude, *p*, given by Equation (7.1) is 63.4°. From

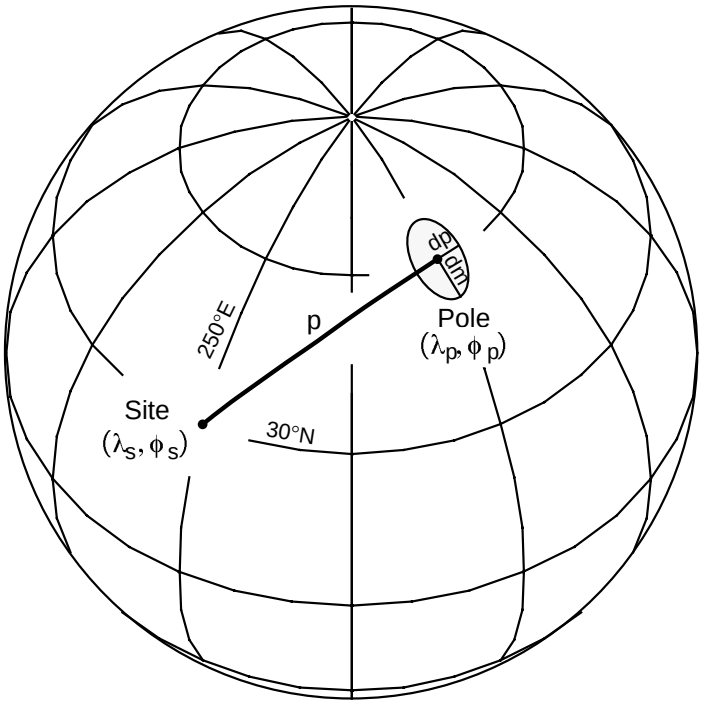

Figure 7.2 Ellipse of confidence about magnetic pole position. *p* is the magnetic colatitude; *dp* is the semi-axis of the confidence ellipse along the great-circle path from site to pole; *dm* is the semi-axis of the confidence ellipse perpendicular to that great-circle path. The projection (for this and all global projections to follow) is orthographic with latitude and longitude grid in 30° increments.

Equation (7.2), the pole latitude, λ_p, is 67.8°N, and the angle β from Equation (7.3) is 86.2°. The product $\sin \lambda_s \sin \lambda_p = 0.463$, while $\cos p = 0.448$, so $\cos p < \sin \lambda_s \sin \lambda_p$, and the pole longitude is given by Equation (7.7) as $\phi_p = 342.7^{o}$E. The pole is illustrated in Figure 7.2. Using Equations (7.8) and (7.9), the confidence ellipse about the pole has $dp = 4.0°$ and $dm = 6.3°$.

TYPES OF POLES

The calculation scheme just described yields the position of the north geomagnetic pole, assuming that the observed direction is produced by a geocentric dipole. But from Chapter 1, we know that the geomagnetic field is more complex than a simple geocentric dipole. The present geomagnetic field is composed of a dominant dipolar field and a higher-order nondipole field. In addition, we know that the geomagnetic field changes with time. To deal with these spatial and temporal complications, various types of magnetic poles have been defined. These magnetic poles are determined from different kinds of observations, and the distinctions between them are important.

Geomagnetic pole

For the present geomagnetic field, it is possible to examine globally distributed observations and determine the best-fitting geocentric dipole. The pole position of that best-fitting dipole is the *geomagnetic pole*. For the year 1980, the north geomagnetic pole was located at approximately 79°N, 289°E in the Canadian Arctic Islands.

For determination of the geomagnetic pole position, globally distributed observations are required to "average out" the nondipole field. An observation of the magnetic field direction at a single location cannot be used because the observed direction would, in general, be affected by the nondipole field. Thus a pole position calculated on the basis of a single observation at a particular location is not expected to coincide with the geomagnetic pole. For example, the present magnetic field direction in Tucson, Arizona ($\lambda_s \approx 32°$N, $\phi_s \approx 249°$E) is $I \approx 60°$, $D \approx 14°$, and the resulting pole position is $\lambda_p \approx 76°$N, $\phi_p \approx 297°$E, substantially removed from the present geomagnetic pole.

Virtual geomagnetic pole

Any pole position that is calculated from a single observation of the direction of the geomagnetic field is called a *virtual geomagnetic pole* (abbreviated VGP). This is the position of the pole of a geocentric dipole that can account for the observed magnetic field direction at one location and at one point in time. As in the example above, a VGP can be calculated from an observation of the present geomagnetic field direction at a particular locality. If VGPs are determined from many globally distributed observations of the present geomagnetic field, these VGPs are scattered about the present geomagnetic pole. In paleomagnetism, a site-mean ChRM direction is a record of the past geomagnetic field direction at the sampling site location during the (ideally short) interval of time over which the ChRM was acquired. Thus a pole position calculated from a single site-mean ChRM direction is a virtual geomagnetic pole.

Paleomagnetic pole

Because of nondipole components, a site-mean VGP is not expected to coincide with the geomagnetic pole at the time the ChRM was acquired. In theory, the geomagnetic pole in ancient times could be determined by paleomagnetic investigation of globally distributed rocks of equivalent age. In practice, dating techniques are sufficiently precise to allow such geomagnetic pole determinations only for the past few thousand years (see Figure 1.9). This direct technique obviously could not be extended to rocks older than about 5 Ma because continental drift has changed the relative positions of observing localities. The only practical solution to averaging out effects of the nondipole field is to time average the field for an interval of time covering the periodicities of secular variation of the nondipole field. As discussed in Chapter 1, periodicities of secular variation of the nondipole field are dominantly less than 3000 yr.

Analyses presented in Chapter 1 also indicate that the dipolar geomagnetic field undergoes secular variation, causing the geomagnetic pole to random walk about the rotation axis with periodicities dominantly from 10^3 to 10^4 yr. The *geocentric axial dipole hypothesis* (briefly introduced in Chapter 1 and examined in detail in Chapter 10) states that, if geomagnetic secular variation has been adequately sampled, the average position of the geomagnetic pole coincides with the rotation axis. Thus a set of paleomagnetic sites magnetized over about 10^4 to 10^5 yr should yield an average pole position (average of site-mean VGPs) coinciding with the rotation axis. Pole positions calculated with these criteria satisfied are called *paleomagnetic poles*. The term paleomagnetic pole implies that the pole position has been determined from a paleomagnetic data set that has averaged geomagnetic secular variation and thus gives the position of the rotation axis with respect to the sampling area at the time the ChRM was acquired.

Procedures for calculating paleomagnetic poles have changed during the past decade. Previously, the approach was to calculate a *formation-mean direction* by using Fisher statistics to average the site-mean directions from a geological formation. The formation-mean direction then was used to calculate the paleomagnetic pole (Equations (7.1) through (7.7)). A 95% confidence ellipse for the paleomagnetic pole was determined from the α_{95} circle about the formation-mean direction (Equations (7.8) through (7.9)). This pole position was reported as the paleomagnetic pole from the formation, and the error ellipse was used as an estimate of precision.

As shown above, the α_{95} circle of confidence about a mean direction is mapped by the dipole formula into an ellipse of confidence about the calculated pole. Similarly, a circular distribution of directions is mapped into an elliptical distribution of VGPs calculated from those directions. But conversely, a circular distribution of VGPs implies that the distribution of directions yielding those VGPs is elliptical. So site-mean directions or site-mean VGPs (but not both) might be circularly distributed about their respective means. Analyses of large paleomagnetic data sets (from rocks up to a few million years in age) indicate that distributions of site-mean VGPs are more nearly circularly distributed about the mean pole position than are site-mean directions about the formation-mean direction. Consequently, most paleomagnetic poles are now determined in the following manner: (1) From each site-mean ChRM direction, a site-mean VGP is calcu-

lated. (2) The set of VGPs then is used to find the mean pole position (paleomagnetic pole) by Fisher statistics, treating each VGP as a point on the unit sphere. The procedure for determining the mean pole position is the same as for determining a mean direction (Equations (6.12) through (6.15)) except that VGP latitude is substituted for inclination and VGP longitude for declination.

Estimates of (between-site) dispersion of the site-mean VGPs are obtained by using the same procedures applied to directions (Equations (6.16) through (6.22)). But in this case, N = number of site-mean VGPs; R = vector resultant of the N site-mean VGPs; and the confidence limit applies to the calculated mean pole position. An informal convention has developed in which upper-case letters are used for dispersion estimates of VGPs. K is the best-estimate of the precision parameter κ for the observed distribution of site-mean VGPs; S is the angular dispersion of VGPs (estimated angular standard deviation of VGPs) and is usually estimated by Equation (6.18) or (6.19); A_{95} is the radius of the 95% confidence circle about the calculated mean pole (the true mean pole lies within A_{95} of the calculated mean pole with 95% confidence).

Figure 7.3 illustrates an example of a paleomagnetic pole (and A_{95} confidence circle) determined from a set of site-mean VGPs. The example is from the Early Jurassic Moenave Formation of northern Arizona

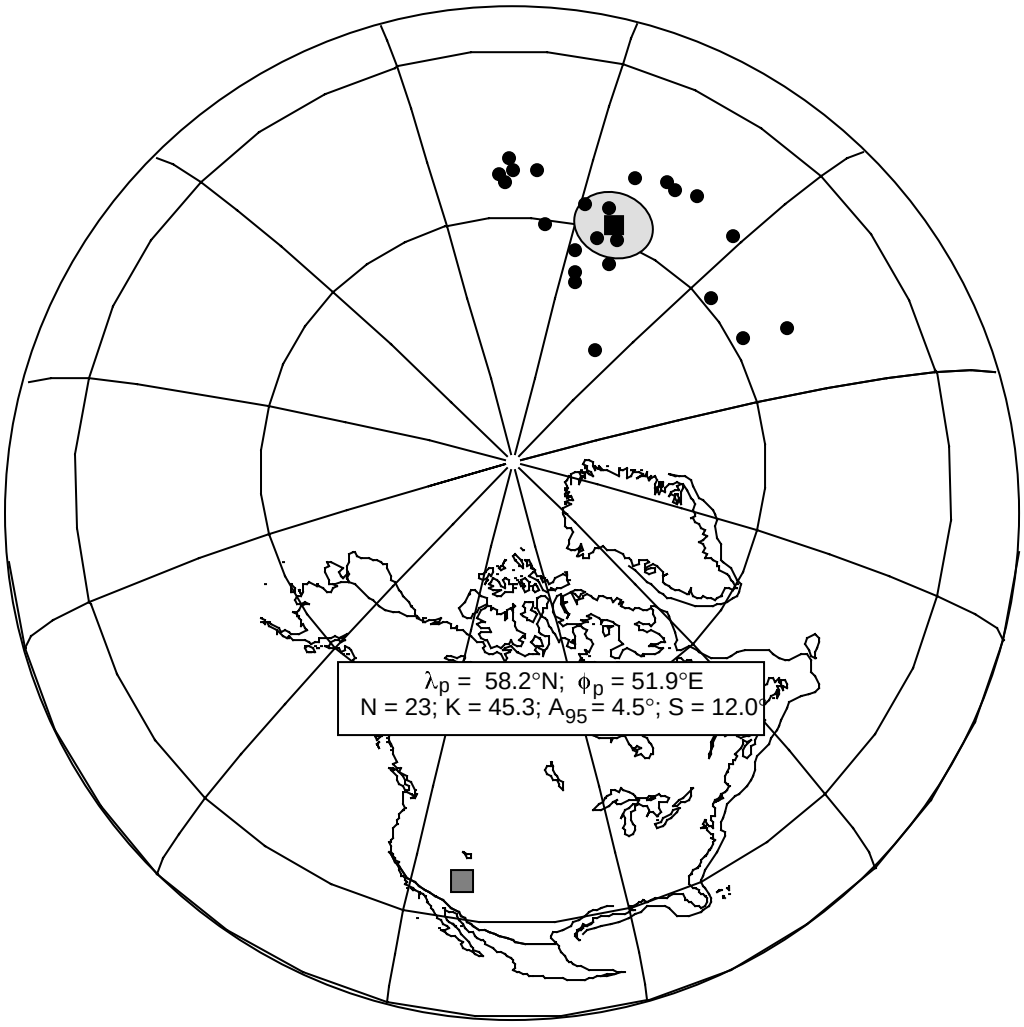

Figure 7.3 Paleomagnetic pole from the Moenave Formation. Solid circles show the 23 site-mean VGPs averaged to determine the paleomagnetic pole shown by the solid square; the stippled circle about the paleomagnetic pole is the region of 95% confidence with radius A_{95}; the region of sampling is shown by the stippled square; the inset gives the location of the paleomagnetic pole along with statistical parameters.

and southern Utah. This formation is dominated by red and purple-red sediments, and an example of thermal demagnetization behavior was provided in Figure 5.7a. For most of the 23 sites from which a ChRM was successfully isolated, the site-mean α_{95} was <10°. Four sites have reversed-polarity ChRM, while 19 sites have normal polarity, and the normal- and reversed-polarity groups pass the reversals test. The mean pole position calculated from the 23 site-mean VGPs is λ_p = 58.2°N, ϕ_p = 51.9°E. The statistical quantities for this collection of site-mean VGPs are K = 45.3, S = 12.0°, and A_{95} = 4.5°.

SAMPLING OF GEOMAGNETIC SECULAR VARIATION

From the discussion of within-site dispersion in the last chapter, it is clear that tightly clustered ChRM directions from multiple samples within a site are desired. Small within-site dispersion and α_{95} imply that the site-mean direction and site-mean VGP are precisely known. However, the situation for dispersion of site-mean VGPs used for determining a paleomagnetic pole is different because sampling of geomagnetic secular variation is involved. Very low between-site dispersion is usually not the desired result.

For a collection of site-mean VGPs to provide an accurate measure of the time-averaged geomagnetic field, those VGPs must represent a sampling of the geomagnetic field over a time interval that exceeds the dominant periodicities of secular variation. From analyses of the Recent geomagnetic field, we know that the dominant periodicities of secular variation are $\leq 10^5$ yr. Thus a collection of paleomagnetic sites that had randomly sampled the geomagnetic field over 10^5 or 10^6 yr ought to average secular variation. A data set that accomplishes this task will have considerable scatter (see below). It is often difficult or impossible to know the precise time interval represented by collections of ancient rocks. Dating techniques might provide an estimate of the age of the sequence (e.g., 260 ± 15 Ma) but in general cannot provide accurate information about the time interval represented. Thus, judging the adequacy of sampling of geomagnetic secular variation must be done in an indirect fashion.

A considerable amount of information about geomagnetic secular variation has been gathered from examination of (1) the historic geomagnetic field, (2) archeomagnetic data covering the past few thousand years, (3) paleomagnetism of lake sediments, and (4) paleomagnetism of dated igneous rocks. Reasonably detailed records of geomagnetic secular variation are available for the past few thousand years. These provide information about the amplitude, periodicities, and spatial variation of Holocene geomagnetic secular variation. Although of lesser fidelity, considerable information about secular variation during the past 5 m.y. is also available. With still less fidelity, records of geomagnetic secular variation are available for the entire Phanerozoic and even into the Precambrian. From this information, the amount of angular dispersion in a paleomagnetic data set that has adequately sampled secular variation can be estimated.

Paleosecular variation

In an attempt to understand fundamental properties of the geomagnetic field, models of geomagnetic secular variation have been developed. Development and analysis of these models for past geomagnetic fields are referred to as *paleosecular variation*, and this subject has important implications for determination of paleomagnetic poles.

A recent analysis of paleosecular variation for the past 5 m.y. is summarized in Figure 7.4. Paleomagnetic data from 2382 lava flows in the 0 to 5 Ma age range were compiled and analyzed. Sampling sites are distributed spatially and temporally to represent a very thorough sampling of the geomagnetic field during the past 5 m.y. Data were screened to ensure that the individual site-mean results are precisely determined, and data were grouped in bands of site latitude. (For this age range, dispersion introduced by lithospheric plate motion is insignificant.)

There are two fundamental observations from Figure 7.4:

1. The dispersion of VGPs is well constrained to the range $10° < S < 20°$.

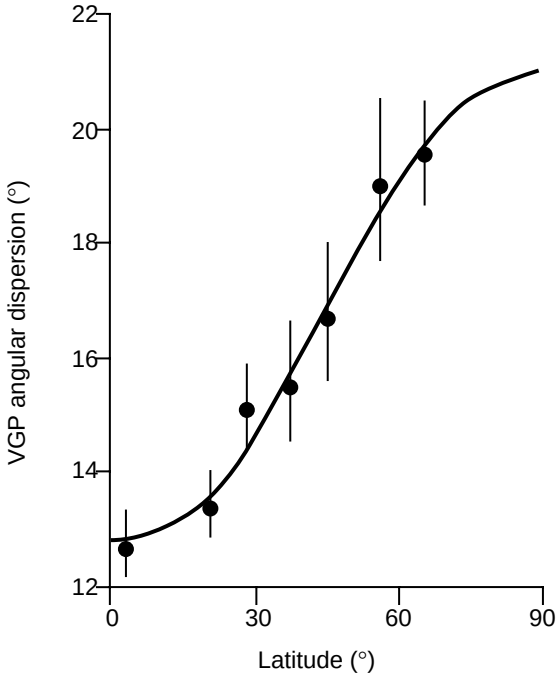

Figure 7.4 Global compilation of paleosecular variation during past 5 m.y. Each data point gives the angular dispersion of VGPs averaged over a band of latitude centered on the data point; the error bars are the 95% confidence limits; the smooth curve is a fit of the observations to a model of paleosecular variation. Redrawn from Merrill and McElhinny (1983).

2. The amount of dispersion of VGPs depends on the site latitude, increasing by almost a factor of two from equator to pole. At least for rocks with ages of 0 to 5 Ma, this analysis provides a powerful and fairly simple method for judging whether a collection of site-mean VGPs from a paleomagnetic study has adequately sampled geomagnetic secular variation.

But what is known about paleosecular variation in more remote geological times? For Late Cretaceous and Cenozoic, seafloor spreading histories allow motion histories of major plates to be reconstructed. The paleomagnetic data available from those plates can be used to construct a "paleoglobal" view of paleosecular variation. For the interval 5 to 45 Ma, the amplitude of VGP dispersion in all latitude bands is slightly greater than for 0 to 5 Ma, whereas for 45 to 110 Ma, dispersion of VGPs is slightly less than for the past 5 m.y. For example, in the band of latitude centered on 10°, VGP dispersion is ~19° for 5 to 45 Ma and ~12° for 45 to 110 Ma as compared to ~13° for 0 to 5 Ma.

With still less certainty than for the last 110 m.y., the amplitude of VGP dispersion produced by geomagnetic secular variation has been investigated for the entire Phanerozoic. The fundamental finding is that the amplitude of paleosecular variation was low during the Cretaceous normal-polarity superchron (~83–118 Ma) and during the Permo-Carboniferous reversed-polarity superchron (~250–320 Ma) (see Chapter 9), two extended intervals during which no reversals of the dipole field occurred. But even during these intervals of unusually low paleosecular variation, VGP dispersion was ~75% of that for the past 5 m.y. So Figure 7.4 can be used as a rough guide in judging the sampling of geomagnetic secular variation afforded by paleomagnetic investigations of rocks of any age (realizing that changes in VGP dispersion of up to ±40% might have occurred during the Phanerozoic).

Testing a paleomagnetic data set for averaging of secular variation is done by comparing observed dispersion of site-mean VGPs with the predicted dispersion. If secular variation has been adequately sampled, the observed angular dispersion of site-mean VGPs should be consistent with that predicted from Figure 7.4 for the paleolatitude of the sampling sites. If the observed dispersion of site-mean VGPs is much less than predicted from Figure 7.4, then the VGPs are more tightly clustered than expected for adequate sampling of secular variation. A likely explanation is that the paleomagnetic sampling sites did not sample a time interval covering the longer periodicities of secular variation. For example, if 20 lava flows were sampled but the flows were all extruded within a 100-yr interval of time, the time interval sampled is too short to afford

complete sampling of geomagnetic secular variation. Accordingly, the VGP dispersion will be much less than would be predicted from Figure 7.4. The implication is that such a paleomagnetic data set has not provided the time averaging of secular variation required for accurate determination of a paleomagnetic pole.

The opposite situation is presented by a VGP dispersion which is substantially larger than predicted from Figure 7.4. Such an observation indicates that there is a source of VGP dispersion in addition to sampling of secular variation. Perhaps there has been tectonic disturbance within the sampling region or there is difficulty in determining the site-mean ChRM directions. In any case, an observed VGP dispersion that substantially exceeds that predicted from Figure 7.4 is a danger signal indicating that the paleomagnetic data are of questionable reliability.

Holocene lavas of western United States

A detailed examination of the paleomagnetism of Holocene lavas in the western United States was made by Champion (see Suggested Readings). A total of 77 lavas were sampled, with site locations primarily in Arizona, Oregon, and Idaho. The large number of samples per lava (11 to 41) and quite straightforward isolation of the ChRM led to site-mean directions with an average $\alpha_{95} \approx 2°$. The dispersion of site-mean VGPs for these 77 lavas is $S = 12.2°$ (95% confidence limits of 11.0° and 13.8°). This is less than the ~16° predicted by Figure 7.4 for the average site latitude of 43°N. So the total dispersion of site-mean VGPs is slightly less than typical for the global geomagnetic field during the past 5 m.y.

This collection of accurate data from a particular region for the past 10^4 yr provides an opportunity to examine (1) the dispersion of site-mean VGPs expected for a collection of paleomagnetic sites that have adequately sampled secular variation and (2) the effects of increasing the number of sites sampled. These data were used to simulate sampling of secular variation in the following fashion:

1. Random numbers were used to select five of the 77 site-mean VGPs.
2. This set of VGPs was treated as a "synthetic paleomagnetic data set" and was used to calculate a "paleomagnetic pole," A_{95}, and scatter statistics.
3. Additional sites then were selected randomly to yield synthetic data sets totaling 10, 20, and 30 sites, and the procedures above were repeated for each data set. Results are shown in Figure 7.5.

There are two major realizations to gain from this examination:

1. The dispersion of site-mean VGPs visually appears large but is entirely the result of sampling the geomagnetic secular variation. Dispersion of site-mean VGPs in the range $10° < S < 25°$ is expected (indeed required) for a set of sites that has adequately sampled secular variation. This level of between-site VGP dispersion is desired for reliable determination of a paleomagnetic pole.
2. For a collection of paleomagnetic sites that has randomly sampled secular variation, approximately ten sites will be required to achieve a confidence limit $A_{95} \leq 10°$. For many purposes (including most tectonic applications), this level of precision is desired. Also N (number of sites) ≥ 10 is required for reasonably accurate estimation of the angular dispersion of VGPs.

EXAMPLE PALEOMAGNETIC POLES

In this section, examples of paleomagnetic poles are introduced, starting with poles that are considered very reliable and progressing to poles that are less well determined. These examples put into practice various principles for evaluating paleomagnetic data that have been outlined in this and previous chapters. Emphasis is placed on the paleomagnetic aspects of these example studies with uncertainties about geological interpretation receiving less attention.

Paleocene intrusives of north-central Montana

Diehl and others (see Suggested Readings) conducted a paleomagnetic study that provides a very reliable paleomagnetic pole. In terms of both quantity and quality of paleomagnetic data, the resulting

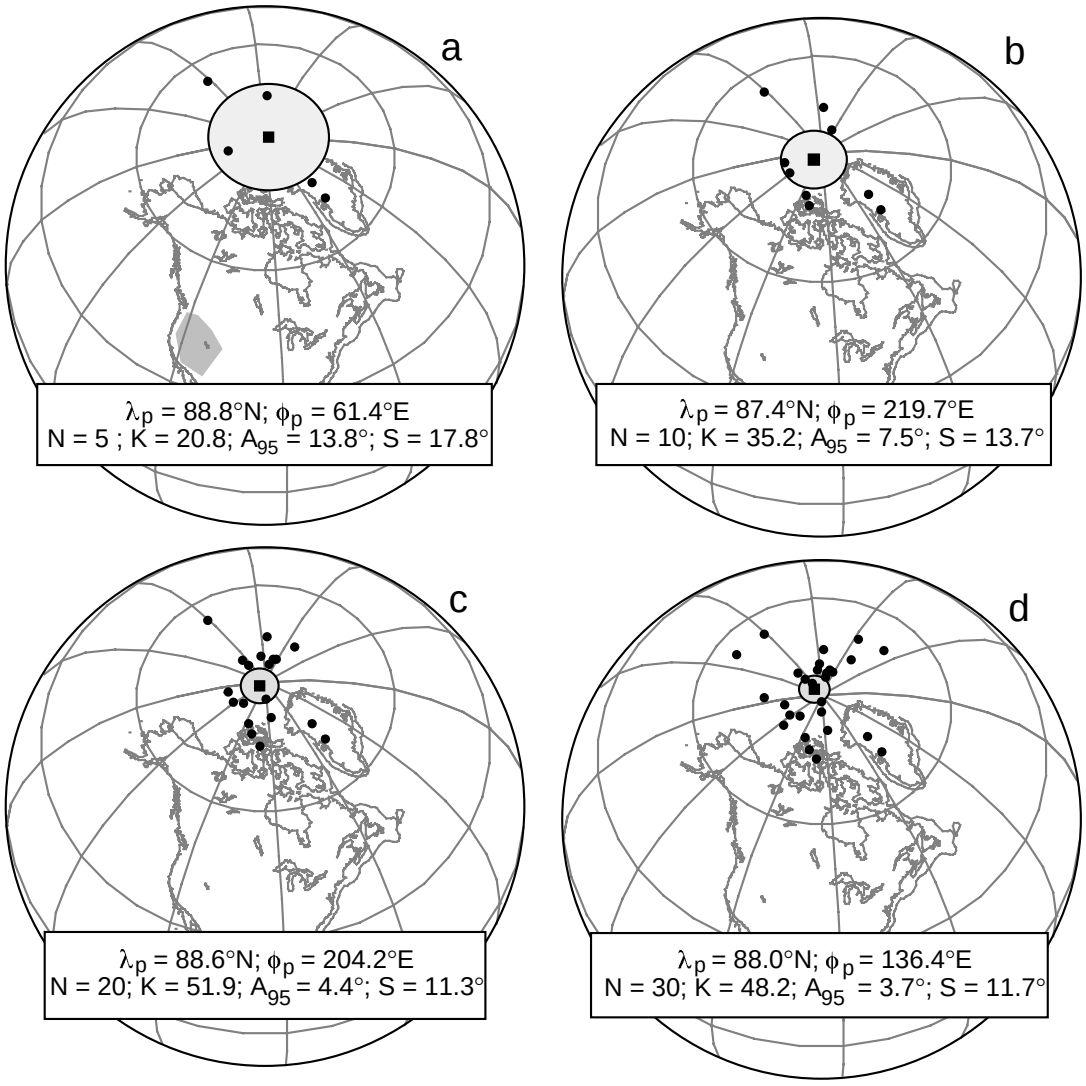

Figure 7.5 "Synthetic paleomagnetic poles" resulting from random sampling of an extensive set of paleomagnetic data from Holocene lavas of the western United States. In each figure, the solid circles show the site-mean VGPs averaged to determine the "paleomagnetic pole" shown by the solid square; the stippled circle about the paleomagnetic pole is the region of 95% confidence with radius A_{95}; the inset gives the location of the paleomagnetic pole along with statistical parameters. (**a**) Synthetic paleomagnetic pole resulting from randomly selecting five VGPs; the region of sampling is shown by the stippled polygon. (**b**) Synthetic paleomagnetic pole resulting from randomly selecting ten VGPs. (**c**) Synthetic paleomagnetic pole resulting from randomly selecting 20 VGPs. (**d**) Synthetic paleomagnetic pole resulting from randomly selecting 30 VGPs. Data from Champion (1980).

paleomagnetic pole for the Paleocene of North America is generally regarded as unusually well determined.

Numerous radiometric dates establish the age of shallow level alkalic igneous intrusions in the Judith Mountains, Mocassin Mountains, and Little Rockies Mountains as Paleocene. These rocks intrude essentially flat-lying older sedimentary rocks. Forty-one paleomagnetic sites were collected, with a minimum of eight separately oriented cores per site. Secondary components of NRM were generally easily erased with ChRM isolated over a wide range of AF demagnetizing fields. ChRM was successfully isolated in 36 of the 41 sites, and 32 of these had site-mean ChRM directions with $\alpha_{95} < 10°$. Five sites had reversed polarity

with the normal- and reversed-polarity groups passing the reversals test for paleomagnetic stability. The ChRM is clearly a primary TRM formed during original cooling of these igneous rocks.

The site-mean VGPs are illustrated in Figure 7.6. For reversed-polarity sites, antipodes of site-mean directions were used to calculate VGPs. The resulting paleomagnetic pole is illustrated along with the confidence circle of radius A_{95} about the pole. Statistical quantities calculated from the set of site-mean VGPs are listed on Figure 7.6. The 17.8° dispersion of site-mean VGPs compares favorably with $S \approx 17°$ predicted by Figure 7.4 for the paleolatitude of ~45°. This observation indicates that the dispersion of site-mean VGPs is consistent with adequate sampling of geomagnetic secular variation. Because both normal- and reversed-polarities of ChRM were observed, the time interval of intrusion must have covered at least parts of two polarity intervals.

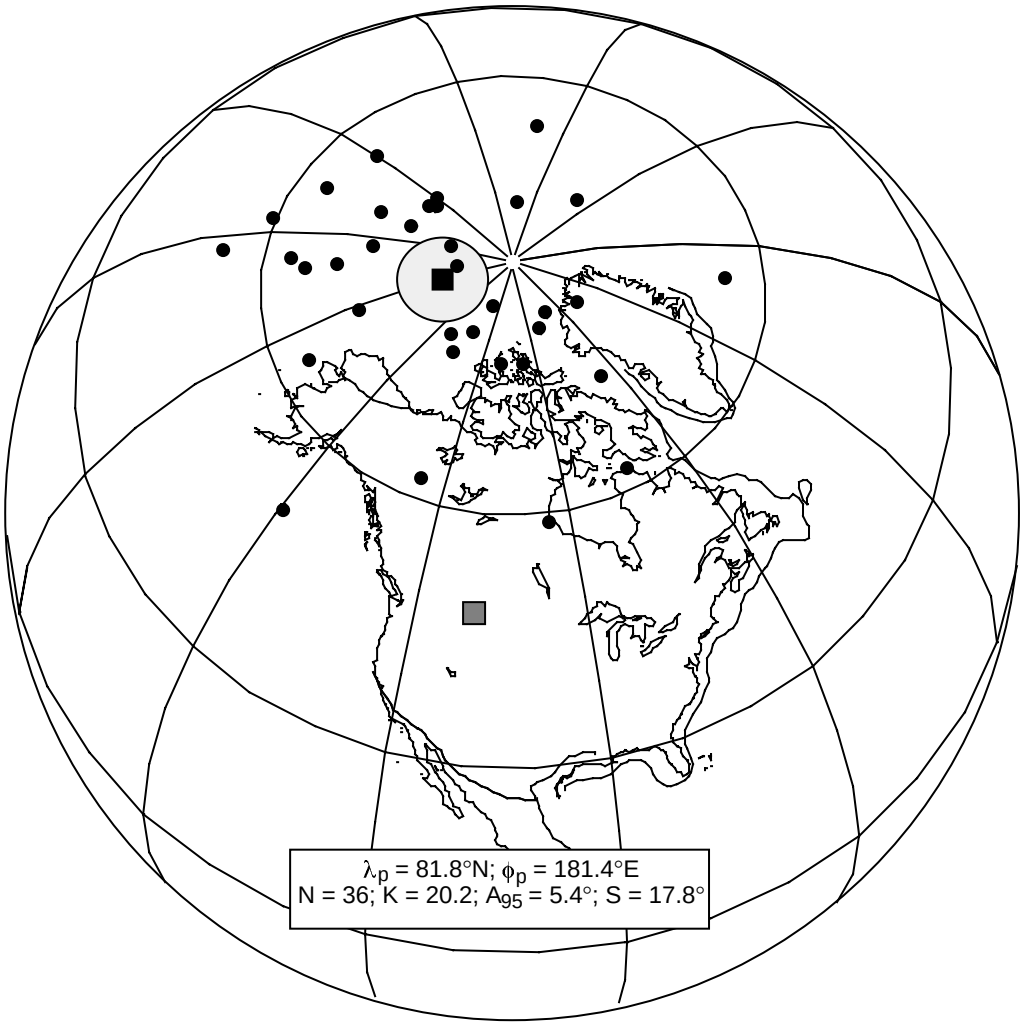

Figure 7.6 Paleomagnetic pole from Paleocene intrusives of north-central Montana. Symbols as in Figure 7.3.

Numerous desirable elements for a paleomagnetic pole determination are present in this investigation. Criteria for accurate determination of site-mean ChRM directions outlined in Chapters 5 and 6 are satisfied. A reversals test for paleomagnetic stability is passed and, along with other data, indicates that the ChRM is a primary TRM, and the large number of sites provides a robust estimation of site-mean VGP dispersion that is consistent with adequate sampling of secular variation. This paleomagnetic study thus provides a reliably determined paleomagnetic pole for the Paleocene of North America, and the A_{95} confidence limit is a realistic assessment of the precision with which that pole has been determined.

Jurassic rocks of southeastern Arizona

A paleomagnetic pole of "intermediate" reliability was determined from Middle Jurassic volcanic and volcaniclastic rocks of southeastern Arizona (reference in Suggested Readings). Nineteen sites with an average of seven cores per site were collected at Corral Canyon in the Patagonia Mountains. Isotopic data indicate an age of 172 ± 6 Ma. Some volcanic units contained magnetite as the dominant ferromagnetic mineral, while hematite dominated in more oxidized volcanic units and there was a single site in red mudstone.

For sites with magnetite as the dominant carrier of NRM, AF demagnetization revealed the same ChRM direction as did thermal demagnetization. For sites with hematite carrying the NRM, thermal demagnetization was generally successful in isolating the ChRM. However, evidence of lightning-induced IRM was found at three sites from which ChRM could not be isolated Directions of ChRM were isolated from the remaining 16 sites. But four site-mean directions were widely divergent from the other 12 site means (by more than two estimated angular standard deviations). Although only speculative explanations could be provided, these four sites probably do not provide records that are typical of the geomagnetic field during the Middle Jurassic and were not used in the determination of the paleomagnetic pole.

Site-mean ChRM directions of the 12 remaining sites were reasonably well determined; eight site-mean directions had $\alpha_{95} < 10°$. One site had reversed polarity with antipode in the middle of the 11 normal-polarity site-mean directions. But with only one reversed-polarity site, rigorous evaluation of the reversals test is not possible. The site-mean VGPs are shown in Figure 7.7 along with the resulting paleomagnetic pole and statistical quantities. The observed dispersion of site-mean VGPs is 11.5°, in reasonable agreement with $S \approx 13°$ predicted from Figure 7.4 for adequate sampling of secular variation.

This paleomagnetic pole is considered of "intermediate" reliability because there are strengths and weaknesses to the paleomagnetic data used in its determination. On the positive side, several aspects of the data indicate that the ChRM directions in these Middle Jurassic volcanic rocks are primary TRM:

1. There is reasonably clear isolation of ChRM directions from numerous volcanic units of variable deuteric oxidation state and from an interbedded sedimentary unit.
2. A reversed-polarity site has ChRM direction antipodal to the grouping of normal-polarity site means.
3. The dispersion of site-mean VGPs is consistent with sampling of geomagnetic secular variation. Collectively, these observations indicate that the ChRM of these volcanic rocks is primary TRM.

On the negative side, data from several sites were rejected because a ChRM could not be isolated or the site-mean ChRM direction was divergent from the dominant clustering of site-mean directions. No matter how well founded such data rejection might be, it always causes some uneasiness with the final result. In the end, just 12 sites proved useful for determination of the paleomagnetic pole. Successful isolation of ChRM directions from more sites might have yielded a more confidently determined pole. However, there are sufficient attributes to this paleomagnetic data to regard the "Corral Canyon Pole" as reasonably well determined and the associated $A_{95} \approx 6°$ as a realistic estimate of the precision.

Two problem cases

Figure 7.8 illustrates "paleomagnetic poles" that suffer from two very different inadequacies in the data used for their determination. In Figure 7.8a, site-mean VGPs from 25 sites in a stratigraphic succession of Paleocene lavas at Gringo Gulch (yes, this is a real place name!) near Patagonia, Arizona, are illustrated. Site-mean ChRM directions were all well determined. But all site-mean ChRM directions have reversed polarity. Furthermore, the dispersion of site-mean VGPs (S) is only 4.1° compared with a predicted dispersion $S \approx 14°$ for the paleolatitude of 30°. The obvious problem here is that the VGPs are too tightly clustered. This suggests that the 25 lavas at Gringo Gulch have not adequately sampled geomagnetic secular variation. These flows most likely were extruded in rapid succession during an interval substantially less than the longer periodicities of secular variation, perhaps $<10^3$ yr.

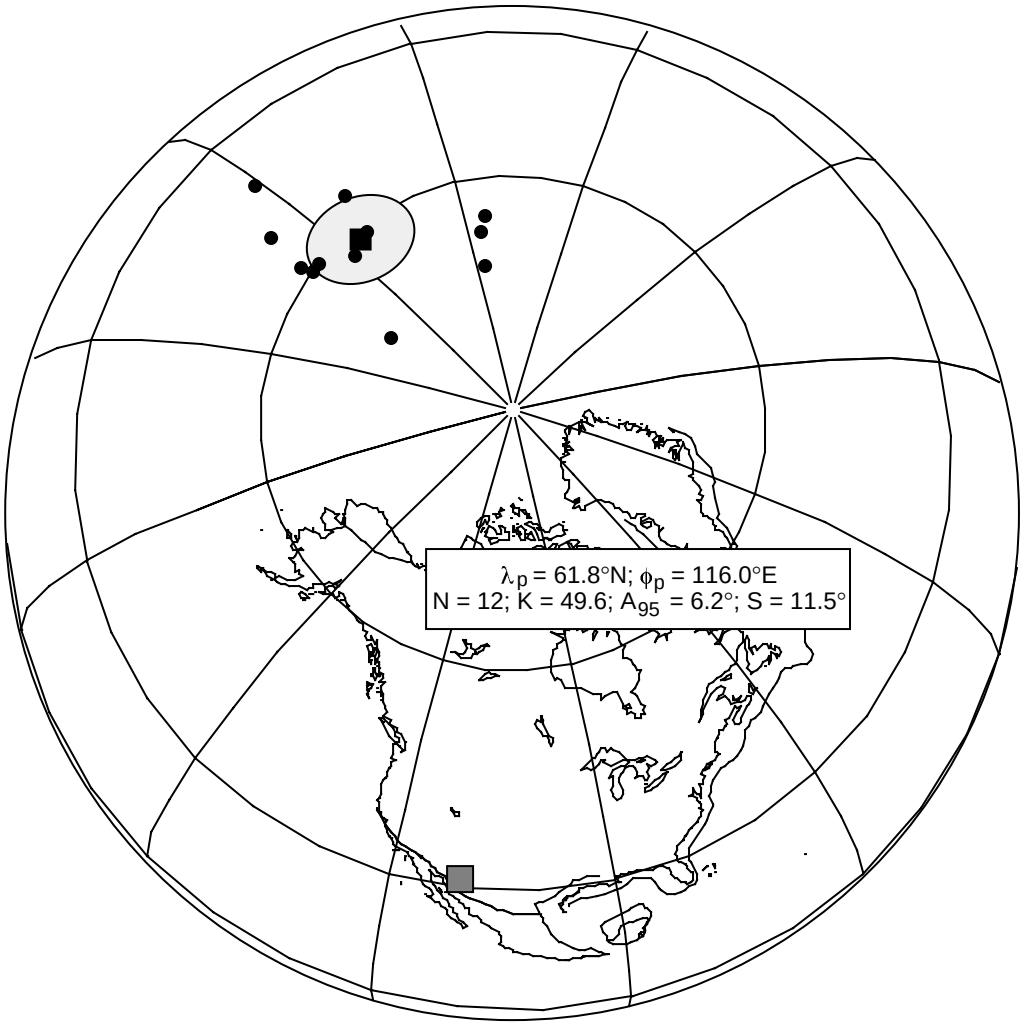

Figure 7.7 Paleomagnetic pole from Middle Jurassic volcanic and volcaniclastic rocks of southeastern Arizona. Symbols as in Figure 7.3.

The small confidence limit (A_{95} = 1.4°) for the calculated pole position gives the impression of a highly accurate paleomagnetic pole determination. In this case, however, the small A_{95} is misleading. The Gringo Gulch pole is not more accurate than the paleomagnetic pole from the Paleocene intrusions of north-central Montana discussed above. On the contrary, the Gringo Gulch pole is not nearly as reliably determined as is the pole from the Montana intrusives. This example indicates the importance of careful data examination (at least at the site-mean level) in judging reliability of paleomagnetic poles.

Because of changing experimental techniques and criteria for determination, there are many "paleomagnetic poles" in the literature that would not today be considered reliably determined. So as not to raise the hackles of the original investigators, the following example from the literature is referred to as the "mystery pole." The paleomagnetic sampling leading to determination of the mystery pole was carried out on volcanic rocks in the southern hemisphere. In the publication reporting the mystery pole, results from 12 sites are listed. However, if one applies data selection criteria requiring three or more samples per site and site-mean $\alpha_{95} \leq 20°$, then data from only three sites remain! Site-mean VGPs for these three sites are illustrated in Figure 7.8b, using the standard convention of showing the paleomagnetic pole closest to the present south geographic pole for observations from the southern hemisphere.

Although the mystery pole has A_{95} = 8.7° and does not at first sight appear poorly determined, again appearances are deceiving. As discussed above, a paleomagnetic data set with only three site-mean direc-

Figure 7.8a Example 1 of a "paleomagnetic pole" based on problematical data. Paleomagnetic pole from Paleocene lavas in southern Arizona. The region of sampling is shown by the stippled square; this paleomagnetic data set has probably not adequately sampled geomagnetic secular variation. Symbols as in Figure 7.3.

tions cannot provide adequate averaging of geomagnetic secular variation. Nor can such a data set provide more than rough estimates of angular standard deviation. Therefore, this paleomagnetic data set does not, in fact, constitute a reliable determination of a paleomagnetic pole. In contrast to earlier examples, the small number of sites prevents rigorous evaluation of the averaging of secular variation.

CAVEATS AND SUMMARY

The principles and discussions above on sampling of geomagnetic secular variation assume that ChRM is acquired within a time interval (generally $\leq 10^2$ yr) that is much shorter than dominant periodicities of secular variation. This assumption is certainly justified for volcanic rocks because they cool through the blocking temperatures of TRM within at most a few years. But for deep-level igneous intrusions (especially plutonic rocks), acquisition of primary TRM may occur over millions of years. This slow cooling can result in time-averaging of the geomagnetic field within-site (even within sample).

An example of this time integration of the geomagnetic field is provided by paleomagnetic studies of Cretaceous plutonic rocks of the Sierra Nevada (see Frei et al. in Suggested Readings). After removing the contribution from within-site dispersion, the between-site dispersion of ChRM directions in three plutonic

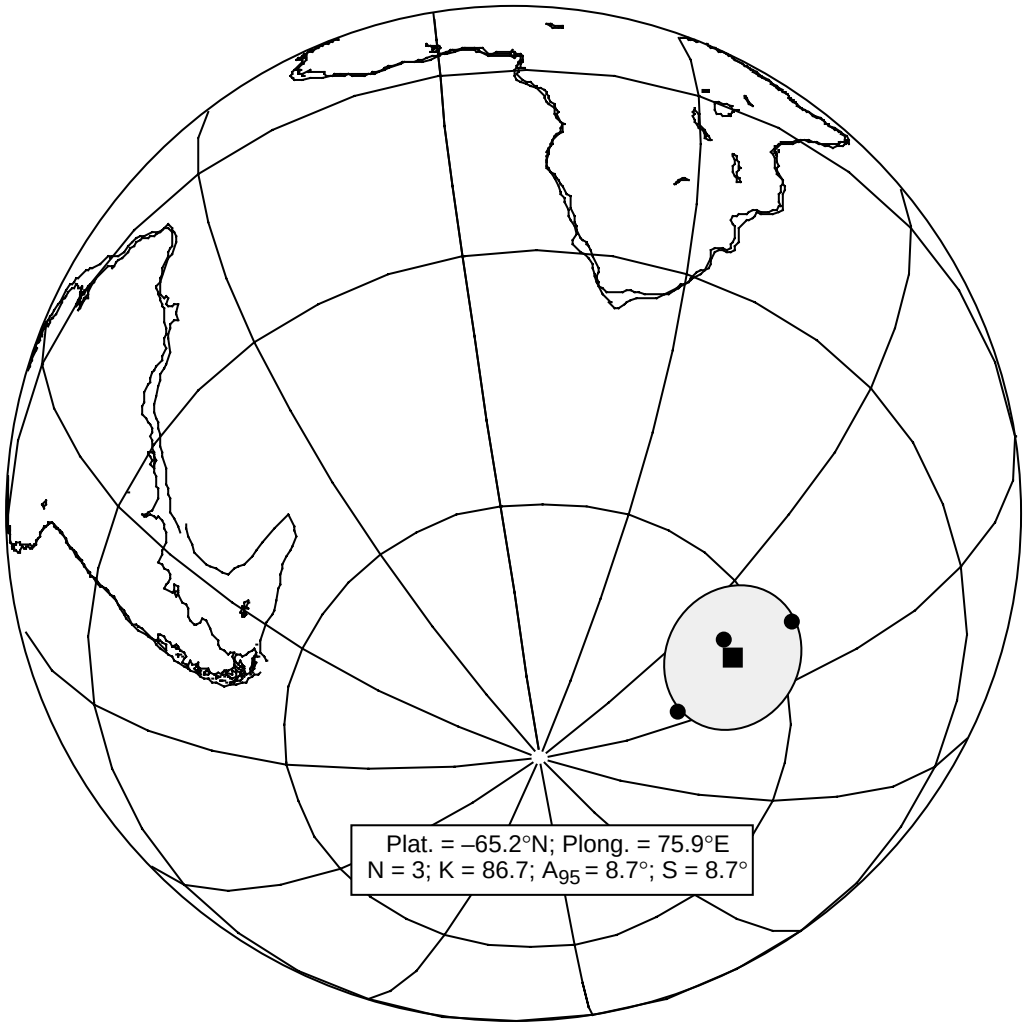

Figure 7.8b Example 2 of a "paleomagnetic pole" based on problematical data. The mystery pole based on just three site-mean VGPs. Symbols as in Figure 7.3.

bodies was found to range from 4.8° to 9.7°. This dispersion is substantially lower than the ~16° expected at the Cretaceous paleolatitude of the Sierra Nevada. This low between-site dispersion is not because the rocks were magnetized in a time interval that was too short to provide adequate sampling of secular variation. Instead, the low dispersion results from intra-site or even intra-specimen time averaging of geomagnetic field direction as these rocks were very slowly cooled through their blocking temperature intervals.

A time integration of the geomagnetic field direction may also occur in sedimentary rocks with slow lock-in of pDRM or in red sediments with protracted CRM acquisition. For any rock units in which ChRM acquisition integrates secular variation over $\geq 10^3$ yr, the dispersion of site-mean VGPs may be substantially less than predicted by Figure 7.4. This should be kept in mind in assessing whether a paleomagnetic data set has adequately sampled secular variation.

For paleomagnetic data from stratigraphic successions of volcanic rocks, the episodic nature of volcanic eruption must be considered. If a sequence of flows is erupted in rapid succession so that no significant secular variation takes place between eruptions, the individual flows in the sequence are not independent samples of the geomagnetic field. For adjacent sites in stratigraphic sections, site-mean ChRM directions should be examined to determine whether those directions are statistically distinguishable. In stratigraphic intervals with indistinguishable site-mean directions, those directions should be averaged and treated as a single sample of the geomagnetic field.

The principles and examples presented in this chapter provide some criteria for evaluation of paleomagnetic data, especially data used to determine paleomagnetic poles. Although each case must be separately evaluated and there are no strict rules, the following are some common-sense criteria:

1. Multiple samples per site (three or more, but preferably six to ten) are highly recommended. Site-mean ChRM should be well defined, as discussed in Chapter 6; site-means with $\alpha_{95} \geq 20°$ would generally be considered unacceptable for inclusion in a data set used for determination of a paleomagnetic pole.
2. Application and rigorous evaluation of field tests of paleomagnetic stability can provide crucial information about timing of ChRM acquisition. Especially for ancient rocks in orogenic zones, field tests can be invaluable.
3. The number of site-mean VGPs used to calculate a paleomagnetic pole should be ten or more. This number is required for reasonable averaging of geomagnetic secular variation and for estimating dispersion of site-mean VGPs.
4. Dispersion of site-mean VGPs should be consistent with adequate sampling of geomagnetic secular variation.

SUGGESTED READINGS

D. E. Champion, Holocene geomagnetic secular variation in the western United States: Implications for the global geomagnetic field, U.S. Geological Survey Open File Report, No. 80-824, 314–354, 1980.
Extensive study of Holocene volcanic rocks in western United States on which results of Figure 7.5 are based.

A. Cox, Latitude dependence of angular dispersion of the geomagnetic field, *Geophys. J. Roy. Astron. Soc.*, v. 20, 253–192, 1970.
Discusses dispersion of geomagnetic field directions and of VGPs.

J. F. Diehl, M. E. Beck, Jr., S. Beske-Diehl, D. Jacobson, and B. C. Hearn, Paleomagnetism of the Late Cretaceous–Early Tertiary North-Central Montana Alkalic Province, J. *Geophys. Res.*, v. 88, 10,593–10,609, 1983.
Article reporting the paleomagnetic data used as the basis of Figure 7.6.

E. J. Ekstrand and R. F. Butler, Paleomagnetism of the Moenave Formation: Implications for the Mesozoic North American apparent polar wander path, *Geology*, v. 17, 245–248, 1989.
Article reporting the paleomagnetic pole illustrated in Figure 7.3.

L. S. Frei, J. R. Magill, and A. Cox, Paleomagnetic results from the central Sierra Nevada: Constraints on reconstructions of the western United States, *Tectonics*, v. 3, 157–177, 1984.
This paleomagnetic study provides an example of intrasite time integration of geomagnetic secular variation.

E. Irving and G. Pullaiah, Reversals of the geomagnetic field, magnetostratigraphy, and relative magnitude of paleosecular variation in the Phanerozoic, *Earth Sci. Rev.*, v. 12, 35–64, 1976.
Presents an analysis of magnitude of paleosecular variation as a function of geologic age.

S. R. May, R. F. Butler, M. Shafiqullah, and P. E. Damon, Paleomagnetism of Jurassic rocks in the Patagonia Mountains, southeastern Arizona: Implications for the North American 170 Ma reference pole, *J. Geophys. Res.*, v. 91, 11,545–11,555, 1986.
Article reporting the paleomagnetic pole illustrated in Figure 7.7.

P. L. McFadden, Testing a palaeomagnetic study for the averaging of secular variation, *Geophys. J. Roy. Astron. Soc.*, v. 61, 183–192, 1980.
Presents some advanced statistical techniques for evaluating whether a paleomagnetic data set has averaged secular variation.

R. T. Merrill and M. W. McElhinny, *The Earth's Magnetic Field*: *Its History, Origin, and Planetary Perspective*, 401 pp., Academic Press, London, 1983.
Chapter 6 presents an in-depth analysis of paleosecular variation.

R. W. Vugteveen, A. E. Barnes, and R. F. Butler, Paleomagnetism of the Roskruge and Gringo Gulch Volcanics, southeast Arizona, *J. Geophys. Res.*, v. 86, 4021–4028, 1981.
Paleomagnetic results illustrated in Figure 7.8a were reported in this article.

PROBLEMS

7.1 A paleomagnetic site from a single Oligocene welded ash flow tuff was collected at site location λ_s = 35°N, ϕ_s = 241.2°E. The site-mean ChRM data are N = 8, I_m = –17.9°, D_m = 232.6°, k = 320.0.

a. From these data, calculate the site-mean VGP for this site. *Note*: The magnetic colatitude, p, must be a positive number (it is the great-circle distance from the site to the pole). If you obtain a negative number for

$$p = \cot^{-1}\left(\frac{\tan I_m}{2}\right) = \tan^{-1}\left(\frac{2}{\tan I_m}\right)$$

then

$$p = \tan^{-1}\left(\frac{2}{\tan I_m}\right) + 180°.$$

b. Estimate the semi-axes (*dp*, *dm*) of the ellipse of confidence about this VGP.

7.2 Data summaries are given below for two (hypothetical) latest Carboniferous formations exposed in central Manitoba, Canada. We are considering the use of these data to determine the latest Carboniferous paleomagnetic pole for the North America craton. Examine the data, assuming that the ChRM directions have been determined by state-of-the-art demagnetization techniques; perhaps plot some observations on an equal-area projection; and come to a conclusion about which of the two data sets is most likely to yield a reliable latest Carboniferous paleomagnetic pole. Explain your reasoning and your choice of the more reliable paleomagnetic data set. *Note***:** During the Late Carboniferous through most of the Permian, the geomagnetic field was in a constant state of reversed polarity.

Blue-winged Olive Formation**:** N = 22 sites in flat-lying red sediments; all sites have reversed polarity. Average of the 22 site-mean VGPs:

N = 22, λ_p = 44.6°N, ϕ_p = 123.4°E, K = 34.2, A_{95} = 5.1°.

Muddler Minnow Formation**:** N = 27 sites in basaltic andesite flows; N = 13 normal-polarity sites from flat-lying strata have mean direction:

N = 13, I_m = 15.0°, D_m = 309.0°, k = 27.4, α_{95} = 12.1°

N = 14 reversed-polarity sites from strata with dip azimuth = 317° and dip = 18° have in situ (before structural correction) mean direction:

N = 14, I_m = –52.0°, D_m = 169.0°, k = 24.7, α_{95} = 12.8°